Improved Modeling of Kinematics-Induced Geometric Variations in Extrusion-Based Additive Manufacturing Through Between-Printer Transfer Learning

Jie Ren, An-Tsun Wei, Zhengqian Jiang, Hui Wang, and Xiaolin Wang

***Abstract*— For extrusion-based additive manufacturing, the variation in material deposition can significantly affect printed material distribution, causing infill nonuniformity and defects. These variations are induced by kinematic variations of the printer extruder. Such infill nonuniformity is more significant in an application of collaborative printing systems by which multiple printers' extrudes co-create the same structure since more accelerate–decelerate kinematic cycles are involved. There is a lack of a quantitative understanding of the impact of printing kinematics on such variations to guide the printing process control. This article deals with the challenge by establishing a mathematical model that quantifies the printing width variations along the printing paths induced by printing speed and acceleration. The model provides vital information for predicting infill pattern nonuniformity and potentially enables using G-code adjustment to compensate for the infill errors in future research. In addition, since the model captures the mechanism of kinematics-induced variations, it provides a way of between-printer knowledge transfer on estimating printing errors. This article further proposes an informative-prior-based transfer learning algorithm to improve the quality prediction model for a printer with limited historical data by leveraging the shared data from interconnected 3-D printers. A case study based on experiments validated the effectiveness of the proposed methodology.**

***Note to Practitioners*—This article quantitatively studies the impact of extruder kinematics on geometric variations and printing quality in extrusion-based 3-D printing processes. The model can help predict the geometric printing quality and related defects, such as overfill or underfill problems given kinematics setup by G-code. This study can expedite the learning process of printing variations induced by kinematics for new printers to set up monitoring and G-code adjustment for process control in the early stage of production when the data are limited. In the long run, such between-printer transfer learning has the potential to enable the transfer learning for interconnected collaborative 3-D printing systems with improved printing efficiency and quality.**

***Index Terms*— Additive manufacturing (AM), geometric variations, printing kinematics, quality control, transfer learning.**

I. Introduction

EXTRUSION-BASED additive manufacturing (AM), also known as fused filament fabrication (FFF) or fused deposition modeling (FDM), is a cost-effective flexible manufacturing method of building 3-D parts by adding materials layer-by-layer. However, one key barrier that prevents extrusion-based AM from being applied to more industrial applications is the relatively low fabrication quality in dimensional accuracy and mechanical strength.

The quality control can be regarded as one of the major challenges in FDM processes [1], [2]. The printing quality can significantly affect the mechanical properties. Poor printing accuracy can lead to excessive amounts of workload for the postprocessing of printed parts or assembly failure. In the emerging applications of FDM [3], the printing accuracy plays a more important role, such as the printing of tooling and molds for composite structure forming (e.g., car hood or body made by carbon fiber composite).

Abundant research has been conducted on the quality modeling and control of AM. A large body of literature focused on the quality control for printing that uses laser or light, e.g., stereolithography (SLA) [4]–[8]. For the product dimensional accuracy of the extrusion-based AM, several material-shrinkage models were proposed to characterize the product geometric deviations for different product shapes [9], [10]. A neural network model was developed to study the effect of product shape design parameters on its dimensional accuracy [11]. In addition, research also addressed the influence of process parameters on the product quality including: 1) dimensional accuracy [12]–[14];

Manuscript received September 12, 2020; revised December 6, 2020 and February 7, 2021; accepted February 18, 2021. This article was recommended for publication by Associate Editor Y. Liu and Editor J. Li upon evaluation of the reviewers' comments. This work was supported by NSF under Grant CMMI-1901109 and Grant HRD-1646897. *(Corresponding author: Hui Wang.)*

The authors are with the Department of Industrial and Manufacturing Engineering, FAMU-FSU College of Engineering, Tallahassee, FL 32310 USA (e-mail: hwang10@fsu.edu).

Color versions of one or more figures in this article are available at https://doi.org/10.1109/TASE.2021.3063389.

Digital Object Identifier 10.1109/TASE.2021.3063389

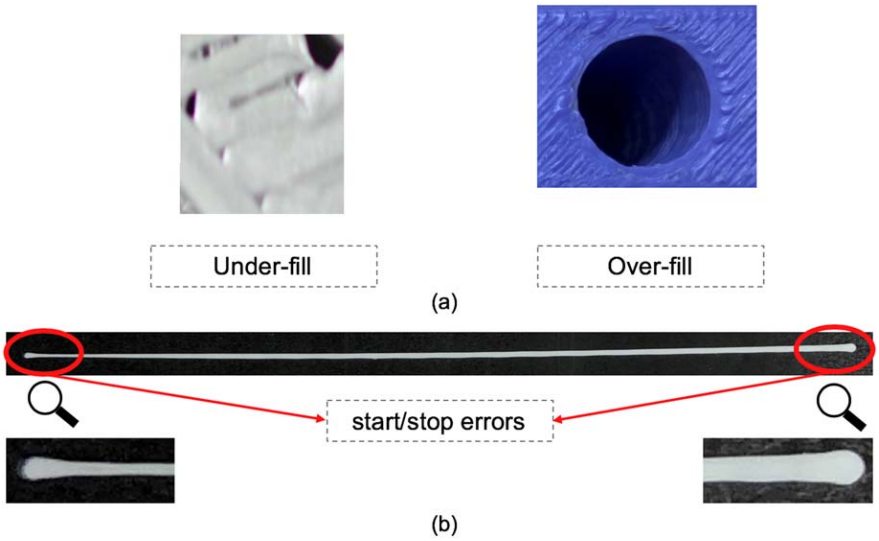

Fig. 1. (a) Kinematics induced quality problems, underfill and overfill defects. (b) Printing errors at the start and stop end of the printed lines.

2) the relationship between process parameters and mechanical properties, e.g., tensile strength [15]; 3) the surface roughness characterization based on process parameters [16]; and 4) the effect of the *in situ* process variables on the product quality [17].

Most of the prior research focused on identifying the relationship between the process conditions and the overall quality of the final product. For example, prior studies only concerned with the geometric quality, such as the external contour of the printed structure. However, the quality of material filling in the structure is much less addressed. The variation in the material filling patterns can significantly contribute to structural or surface defects such as overfill or that especially occur near the end segments of each printing line. As shown in Fig. 1(a), these problems exhibit nonuniform distributions of filling materials on each layer and can potentially deteriorate the structural integrity and strength and affect the functional performance, thus preventing the widespread application.

The nonuniformity in the material distribution that causes infill defects can be attributed to the variations at two ends of a printing line deposited onto each layer [see Fig. 1(b)]. The printing line is the building block of the entire structure made by extrusion-based AM. When multiple printing lines are deposited side-by-side to create the infill pattern, the filling defects can be induced by such geometric variations in the printing lines. The infill defects are particularly evident when the infill lines reach the shape boundary, where each infill line stops or starts. The dimensional accuracy of a single-printing path affects more sophisticated 3-D printing quality control. The variations of the printing line geometry are mostly caused by extruder kinematics, including printing speed, acceleration, and deceleration. The kinematics can impact the material deposition amount and the width of each printing line as the extruder moves along the printing path. Such infill defects can be more significant in the application of collaborative printing systems, by which multiple printers' extrudes co-create the same structure since more accelerate–decelerate kinematic cycles are involved.

Limited research is available to model the geometric variation of the printing line. Prior research papers [18] had discussed the dimensional error of a single-printing path caused by the start/stop of the nozzle. In the start/stop phases, there might be material overflow or underflow caused by the uncoordinated motion between the liquefier head and the filament roller. Bouhal *et al.* [19] proposed a methodology combining the tool-path tracking strategy and the look-ahead trajectory planning algorithm to improve the printing quality of the 2-D plane by considering not only the contour error induced by the positioning error but also the area of the overfill/underfill induced by the inconsistent flow rates at the start/stop points in the extrusion subsystem. Bellini *et al.* [20] studied the dynamics of the liquefier and established flow control strategies to improve the printing consistency during the printing acceleration/deceleration phases. Ravi *et al.* [21] analyzed the effect of temperature and nozzle-bed distance on the deposition width. Qin *et al.* [22] proposed a speed control algorithm and combined the Hbot kinematic system to increase the smoothness of the feed rates, which reflects the machine's speed fluctuation (acceleration/deceleration) in the tool path of the curve and corner point under the extrusion-based printing. Santana *et al.* [23] demonstrated that the machine repeatability is highly affected by various printing speeds and extrusion temperatures. Comminal *et al.* [24] also built a numerical model to analyze the deposition flow under different printing parameters.

A major challenge to the training of quality prediction models is the limited samples or data. Recent research developed small-sample modeling or the transfer learning methods by leveraging the knowledge from other data sources. The deviation error of the 2-D printing shape is usually decomposed into shape-independent error (SIE) and shape-specific error (SSE). Cheng *et al.* [25], [26] modeled the two types of errors and combined not only the parameter-based transfer learning for SIE but also the feature-based transfer learning for SSE to estimate the in-plane freeform shape accuracy. By SSE modeling, even the multiple distinct shapes can still jointly

estimate the shape deviation from the similar local features. Sabbaghi *et al.* [27] also introduced Bayesian modeling to approximate the global-and-local in-plane shape error from the polygon based on the limited cylinder shape data in AM. It is also not necessary that transfer learning needs to be implemented under the same experimental conditions. The recent AM transfer learning study proposed the effect equivalence framework to characterize the discrepancy between two different processes [28] or materials [29] and estimated the total equivalent amount of the lurking variables by the Bayesian method. The estimated total equivalent amount will be transferred as an input in the error compensation modeling.

When a new printer is engaged in printing, there is limited time or cost for a new printer to fabricate products under different kinematics or G-codes. Leveraging the experiences and knowledge from an existing printer with more historical quality data can be an effective solution to supplement the information. Although the existing printer with rich historical data can have different kinematics characteristics, size, or weight from the new printers, the impact of process setup on printing line quality can still be similar, thereby creating an opportunity of between-printer transfer learning. Nevertheless, applying state-of-the-art transfer learning for AM to capture how extruder kinematics impact printing quality has the following limitations.

The related studies on transfer learning and the shape error modeling based on small samples in AM all focused on the shape variation/deviation versus nominal shapes on computer-aided design (CAD) models. Based on this line of methodology, the shape errors can be compensated for by adjusting the CAD model to offset the observed or predicted errors. However, the impact of printing process conditions, such as extruder's kinematic characteristics (speed and acceleration) and printing temperature, on shape errors is usually not considered in these models. These conditions are usually set up in the G-codes for the printing process. Although the transfer learning approach [29] associates the lurking differences with the effect of the thermal conductivity in the distortion modeling, the adjustment still relies on the offline adjustment of CAD models. State-of-the-art shape error transfer learning did not reveal the process–quality relationship, which is necessary for near real-time process control by adjusting G-codes in future research. In addition, date-driven transfer learning algorithms originally developed in computer science (as reviewed in [30]) fall short of capturing interpretable between-printer relatedness or similarity by exploring the similar covariance structure of the model parameters for the between-printer data.

In summary, the literature review identified the following research gaps, including 1) very limited research that addressed the material filling defects induced by geometric variations in printing lines for extrusion-based printing; 2) a lack of quantitative models to estimate/predict printing line variations given the printer's kinematics setup specified by G-code; 3) a lack of methods to establish such a prediction model with good accuracy for extrusion-based printing based on limited historical data; and 4) a lack of methods to quantify the between-printer relatedness or similarity in an interpretable way to enable the knowledge transfer from data-rich printer to new similar-but-nonidentical printers for the fast training of process control strategies. The transfer learning between the data-rich and new printers is outlined in Fig. 2.

To deal with research gaps (1) and (2), this article quantitatively studies the impact of extruder kinematics on the geometric variation of the printing line by developing a piecewise data model driven by engineering knowledge to quantify the changing trend of the linewidth. To tackle research gap (3), this article employs the data shared between two similar-but-nonidentical printers to allow for the between-printing knowledge sharing that supplements information to improve the modeling accuracy. Such a data sharing scenario commonly exists in an interconnected collaborative AM process, by which 3-D printers can exchange quality data via networks to enhance the final product quality. The idea of multiprinter co-printing has also been materialized by using multiple mobile printers to co-create the same structure [31]. The operation of cooperative 3-D or swarm 3-D printing involving printing path planning or the real-time path monitoring highly requires data sharing between printers by interacting with the host in a client–server pattern [32] to prevent printing arm from collisions. To deal with (4), this article explored the potential between-printers similarity and proposed a shared covariance-based (as an informative prior) parameter estimation method to improve the accuracy of the parameter estimation for a printer that lacks sufficient data. The outcome of this article can provide valuable information to improve the building quality and offer opportunities to implement automatic process control or error compensations by adjusting G-codes for quality improvement.

This article is organized as follows. Following Section I, Section II conducts modeling of the impacts of extruder kinematics as specified in printer G-codes on the printing line variations based on experiments. By using the model, this section develops a transfer learning algorithm to improve the modeling accuracy by exploring the between-printers similarity. Section III demonstrates the effectiveness of the proposed method by experimental data and discusses the potential applications of the proposed model. This article is summarized in Section IV, and future work is outlined in Section V.

II. Improved Modeling of Kinematics-Induced Printing Line Variations Through Between-Printer Transfer Learning

This section first conducts modeling of the impact of kinematic characteristics of the extruder on the width variation of each printing line (see Section II-A). The model serves as a common basis for establishing the between-printer transfer learning about similar variation patterns and improve the modeling accuracy (see Section II-B).

A. Kinematic-Based Printing Linewidth Model of a Single 3-D Printer

For material-extrusion-based AM, G-codes are used to control the movement of the nozzle (extruder or liquefier

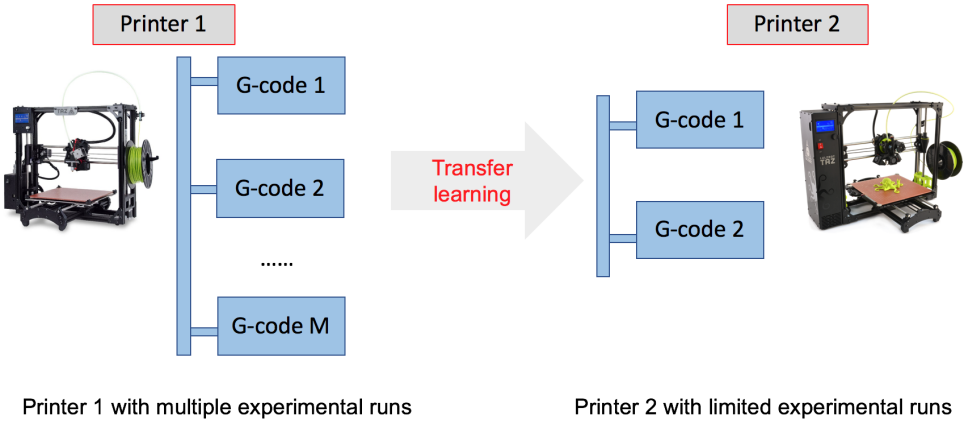

Fig. 2. Transfer learning from a data-rich printer to a similar-but-nonidentical printer with limited data.

head), including jerk, acceleration, and feed. We conducted experiments of a straight-line printing with certain acceleration and feed specified in the G-code. As can be seen in Fig. 1, the start/stop errors are obvious, and its linewidth measurements (captured by a camera) are shown in Fig. 3(a). Also, we can find that the linewidth is closely related to the kinematic status of the nozzle head [see Fig. 3(b)]. Therefore, a model characterizing the relationship between the linewidth and the kinematic parameters, i.e., feed, acceleration, and jerk, can be built. For the simplicity of the model's architecture, the (printing linewidth versus printing length) and (feed versus printing length) are converted to (printing linewidth versus printing time) and (feed versus printing time), respectively. In Fig. 3, the linewidth and feed speed are plotted against both printing length [see Fig. 3(a) and (b)] and nominal printing time [see Fig. 3(c) and (d)]. The printing time in Fig. 3 is the nominal time that can be calculated based on the printing length, jerk, nominal acceleration, and nominal feed that specified in the G-code. However, in the real printing process, the real-time acceleration and feed would have a certain amount of deviations compared with the nominal values specified in the G-code. By considering such deviations, the real acceleration and feed used in the model are assumed to be within a prespecified range as follows:

$$\begin{aligned} a &= r_a a_0 \\ F &= r_F F_0 \\ 0.9 &\le r_a \le 1.1 \\ 0.9 &\le r_F \le 1.1 \end{aligned} \tag{1}$$

where a is the actual acceleration, F is the real target feed speed, a_0 is the nominal acceleration, F_0 is the nominal target feed speed, and r_a and r_F are scaling factors that decide the deviations between real values and specified nominal values. The deviations are usually caused by the printer's internal system errors and material properties. The values of r_a and r_F can be determined via exhaustive grid research. Based on the engineering knowledge and experience, the deviations usually cannot exceed 10% of its nominal target values for the printer with good quality. Therefore, the two parameters were set in the range of 0.9–1.1 for the printer's kinematics. It should be noted that setting a range for these parameters is optional, and the purpose is to narrow the search space to improve the search efficiency. If the quality of the 3-D printers is poor, the range can also be set wider, which will slow the search for prediction model parameters.

By considering that the movement of the printing nozzle usually contains three phases, i.e., accelerating phase, constant speed phase, and decelerating phase, a piecewise model was proposed to characterize the effect of kinematic parameters on printing line quality based on the observations of the experimental relationship of linewidth and printing speed (examples shown in Figs. 3 and 4). For a straight-line printing process, five phases (segmentations) are partitioned as follows (also see Fig. 4).

1) *Phase 1 (p1, Pre-Action Phase):* The nozzle begins moving, and the linewidth decreases.
2) *Phase 2 (p2, Warm-Up Phase I):* The nozzle continues accelerating, and the linewidth starts to increase.
3) *Phase 3 (p3, Warm-Up Phase II):* The nozzle reaches specified feed, and the linewidth keeps increasing.
4) *Phase 4 (p4, Steady Phase):* The linewidth reaches nominal width and remains constant, and the nozzle remains constant speed.
5) *Phase 5 (p5, Slow-Down Phase):* The nozzle starts to decelerate, and the printing linewidth starts to increase.

Compared with the partitions made in [20], the above partitioning separates the warm-up phase into two phases because the time when the printing feed (speed) first reaches its steady state is sometimes ahead of the time when the printing linewidth first reaches a steady state. The breakpoints of the above phases are important for model formulation. To decide the positions of the breakpoints and investigate the relationship of the breakpoints, linewidth, and kinematic parameters, nine experiments with different combinations of nominal acceleration and nominal feed were conducted, as shown in Table I (the jerk is a fixed value of 8 mm/s).

Based on the experiment results, the following conclusions on breakpoints can be drawn.

1) Breakpoint 1 (bp1) is the point where linewidth reaches its minimum value and starts increasing. The time

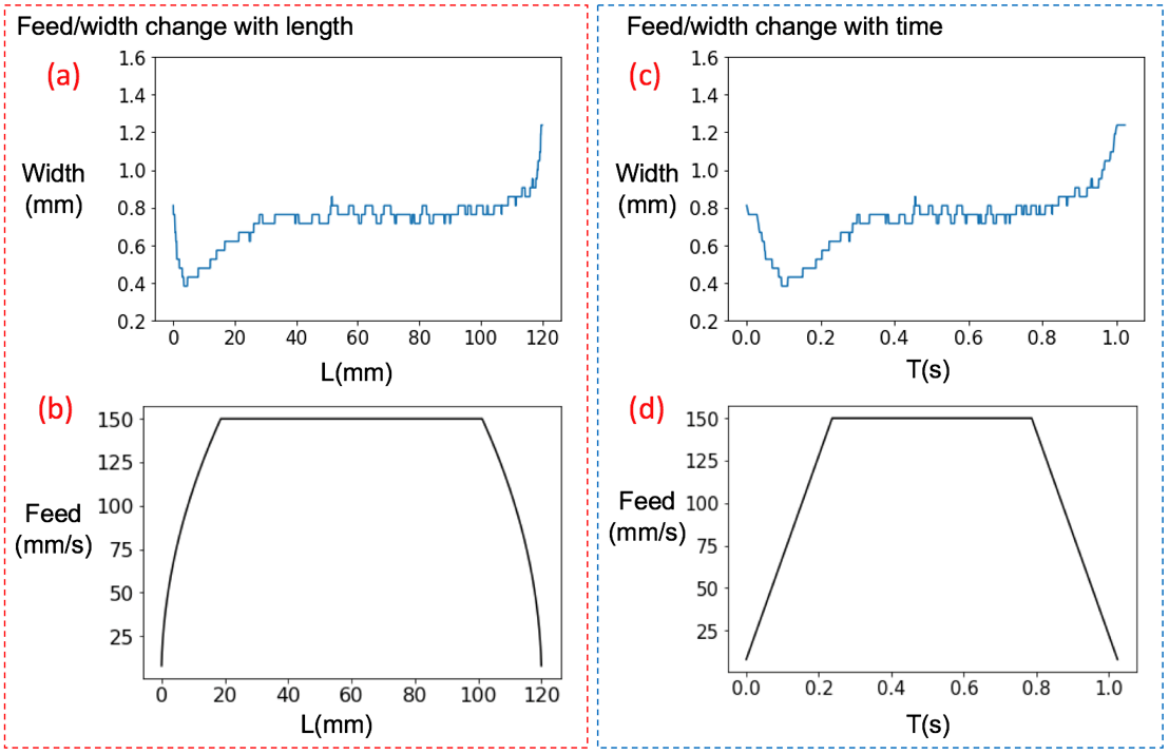

Fig. 3. Feed and linewidth changing with length or time.

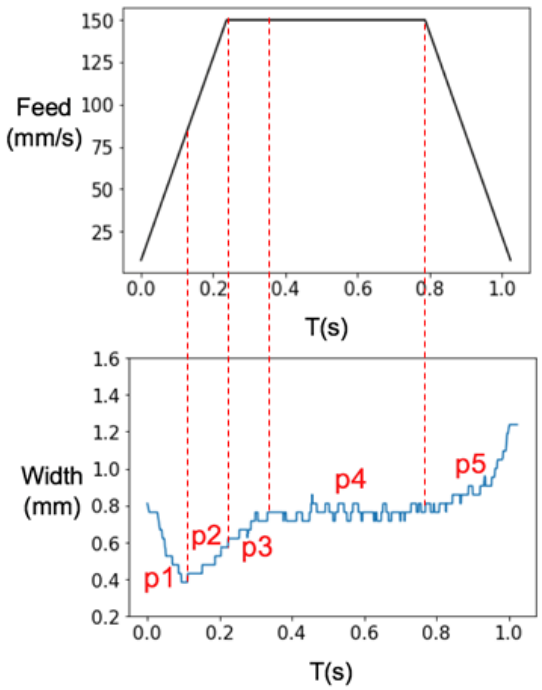

Fig. 4. Five phases of straight-line printing.

position of the point is related to the nozzle acceleration that is shown in Fig. 5.

2) Breakpoint 2 (bp2) is the point where the acceleration phase stops.
3) Breakpoint 3 (bp3) is the point where linewidth first reaches the nominal width.

TABLE I
PRINTING EXPERIMENTS WITH DIFFERENT COMBINATIONS OF FEED AND ACCELERATION

LulzBot Taz 5 Material: PLA Nozzle:0.5mm	Feed (F, mm/s)	Acceleration (a,mm/s^2)
1	150	800
2	100	800
3	50	800
4	150	600
5	100	600
6	50	600
7	150	400
8	100	400
9	50	400

4) Breakpoint 4 (bp4) is the point where the nozzle starts decelerating.

According to the conclusions, bp2, bp3, bp4, and bp5 can be analytically determined by the nozzle motion state, i.e., analyzing the transition points of feed accelerate-constant-decelerate and the linewidth status, i.e., inferring the time when reaches its nominal linewidth. However, bp1 needs to be decided based on nozzle acceleration. The following model (2) can be used to characterize the relationship between bp1 and acceleration with parameters c_0, c_1, and c_2:

$$bp1 = c_0 + c_1 a^{c_2}. \tag{2}$$

The fitted results are shown in Fig. 5. It is worth noting that other models can also describe the relationships between bp1 and acceleration. The proposed model in this section only shows one feasible option. After deciding the breakpoints,

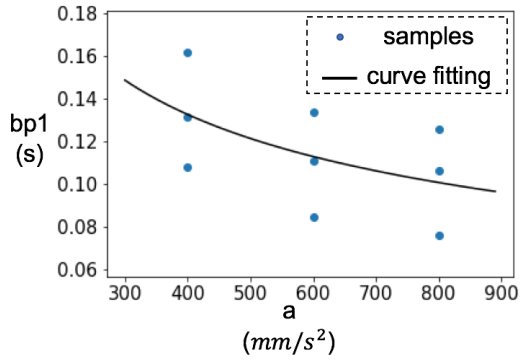

Fig. 5. Breakpoint1 (bp1) versus acceleration.

the models for every phase (segmentations) were proposed as follows:

$$w(t) = \begin{cases} \dfrac{1}{\alpha_1 v(t) + \alpha_2} + e_1, & \text{if } 0 \le t \le bp1 \\ \beta\sqrt{(t - bp1)v(t)a} + w(bp1) + e_2, & \text{if } bp1 < t \le bp2 \\ \gamma\sqrt{(t - bp2)v(t)} + w(bp2) + e_3, & \text{if } bp2 < t \le bp3 \\ c + e_4, & \text{if } bp3 < t \le bp4 \\ \rho \log\left(\dfrac{F}{v(t)}\right) + w(bp4) + e_5, & \text{if } bp4 < t \end{cases} \tag{3}$$

where $w(t)$ is the linewidth at printing time t, $v(t)$ represents the actual nozzle travel speed at time t, a and F are the actual acceleration and the actual target feed speed, respectively [calculated via (1)], $\{\alpha_1, \alpha_2, \beta, \gamma, c, \rho\}$ are unknown parameters, and $\{e_1, e_2, e_3, e_4, e_5\}$ are independent and identically distributed random errors with the normal distribution of $N \sim (0, \sigma^2)$.

Equation (3) is an empirical model based on the experiment results to simplify the model format. It is worth noting that the model in each piece is essentially a linear model in terms of the certain transformation of t, $v(t)$, a, and F (e.g., $(t - bp2)v(t)^{1/2}$ in segment p3). To estimate the parameters $\{\alpha_1, \alpha_2, \beta, \gamma, c, \rho\}$, the maximum log-likelihood estimation or least-squares estimation can be employed for every phase. To simplify the proposed model, we use $\{\theta_i\}_{i=1\ldots6}$ to represent the six parameters $\{\alpha_1, \alpha_2, \beta, \gamma, c, \rho\}$. Thus, the format of the proposed model can be written as $w(t) = X_i\theta_i + w(bp_{i-1}) + e_i$, where e_i is a noise term, if $bp_{i-1} < t \le bp_i$.

To summarize, the model construction consists of the following procedures.

1) Conduct printing experiments with different specified acceleration and feed in G-code and measure the printing linewidth for data collection.
2) Select a pair of values for r_a and r_F from a specified grid as the example shown in (1) to calculate the actual acceleration and target feed speed.
3) Identify the breakpoints based on the linewidth measurements and the kinematic analysis [by using the actual acceleration and target feed speed obtained in step (1)] of the nozzle.
4) Decide the relationship of bp1-acceleration based on the identified bp1 data and the actual acceleration obtained in step (1), i.e., estimate the parameters $\{c_0, c_1, c_2\}$ of (2).
5) Based on the identified breakpoints, partition the experimental data into five data sets.
6) Train the piecewise model for every partitioned data sets, i.e., estimate the parameters $\{\alpha_1, \alpha_2, \beta, \gamma, c, \rho\}$ of (3) and calculate the sum of fitting errors [root-mean-square error (RMSE)].
7) Try a different pair of values of r_a and r_F and repeat the procedures above until exploring the possible pairs of candidate values of r_a and r_F from the specified grid.
8) Select the estimation of $\{r_a, r_F\}$, $\{c_0, c_1, c_2\}$ and $\{\alpha_1, \alpha_2, \beta, \gamma, c, \rho\}$ that has the minimum fitting RMSE as the final optimal model estimation.

For the incoming/new printing processes, the linewidth prediction is made as follows.

1) Calculate the actual acceleration and the actual target feed speed via (1) using the estimated optimal $\{r_a, r_F\}$.
2) Calculate the bp1 using (2) with the estimated optimal $\{c_0, c_1, c_2\}$.
3) Obtain the values of bp2 and bp4 through kinematic analysis.
4) Make piecewise predictions using (3) with the estimate optimal $\{\alpha_1, \alpha_2, \beta, \gamma, c, \rho\}$.
5) Stop estimating p3 when it reaches the target printing linewidth. The cutoff point is bp3.
6) The final prediction is made by connecting p1, p2, p3, p4, and p5 together.

Special cases include the following. First, the printing length might be too short for the nozzle to reach the target feed speed. The movement of the extruder will only have acceleration and deceleration phases, which makes the bp2 and bp4 overlap. In this case, the number of model partitions can be reduced, i.e., only p1, p2, and p5 are considered. Second, the estimated value of bp1 is bigger than that of bp2, i.e., bp2 is in front of bp1. In this case, p2 can be ignored, simplifying (1) to a four-piece model.

The primary purpose of developing the kinematics-quality model is to provide an engineering-driven method to characterize the between-printer relatedness for transfer learning. Traditional data-driven transfer learning usually adopts a high-level abstract data structure, such as kernels or common neural network layers, to capture the shared knowledge between different data sources. The data-driven approach has two disadvantages: 1) the between-printer relatedness lacks engineering interpretation and 2) data-driven approaches usually involve a large number of hard-to-explain model parameters, increasing the model complexity for learning. The engineering-driven model reveals the engineering mechanism regarding the similar impacts of kinematics effects on printed quality among multiple extrusion-based printers. The derived piecewise model is guided by kinematics and has a concise model structure with fewer model parameters, greatly facilitating transfer learning.

Algorithm 1 Estimate Parameter Covariance

Input: K number of experiment samples $\boldsymbol{D} = \{D_1, D_2, \ldots, D_K\}$

Output: Covariance estimation $\hat{\Sigma}_{i,j}$ of two parameters θ_i and θ_j

Procedures:

for D_k in $\boldsymbol{D}$ **do**

Estimate parameter $\theta_i^{(k)}$ and $\theta_j^{(k)}$ independently using maximum log-likelihood estimation or least-squares estimation.

end for

$\hat{\Sigma}_{i,j} = \frac{1}{K-1}\sum_{k=1}^{K}(\boldsymbol{\Theta}^{(k)} - \bar{\boldsymbol{\Theta}})(\boldsymbol{\Theta}^{(k)} - \bar{\boldsymbol{\Theta}})^T$

where $\boldsymbol{\Theta}^{(k)} = [\theta_i^{(k)}, \theta_j^{(k)}]^T$, $\bar{\boldsymbol{\Theta}} = \frac{1}{K}\sum_{k=1}^{K}\boldsymbol{\Theta}^{(k)}$

return $\hat{\Sigma}_{i,j}$

B. Modeling of a Data-Lacking 3-D Printer With Informative Priors Based on Transfer Learning

To obtain a parameter estimation for the linewidth prediction model [see (3)], a sufficient amount of historical data are necessary. However, for a new 3-D printer or a new printing process, there are usually only a limited amount of data, which may not be sufficient to train the model accurately. To address the problem, this section presents a transfer learning method that transfers useful information from the data-rich 3-D printing process to the new data-lacking printing process, by which the modeling accuracy is greatly improved.

To achieve the knowledge transfer, some commonality among different printing processes must be discovered or assumed. For the proposed model [see (3)] since the different phases are from the same printing, it is reasonable to assume the parameters $\{\alpha_1, \alpha_2, \beta, \gamma, c, \rho\}$ of different phases are not independent, i.e., $\{\alpha_1, \alpha_2, \beta, \gamma, c, \rho\} = \theta \sim N(\mu, \Sigma)$. Based on the observations between model coefficients, a further assumption is made that different printers or printing processes share similar parameter covariance structure. Without loss of generality, we assume that printer 1 is the source that contains rich data and printer 2 is the target that lacks data, e.g., $\theta^{(1)} \sim N(0, \Sigma^{(1)})$ and $\theta^{(2)} \sim N(0, \Sigma^{(2)})$, where $\Sigma^{(1)} = q\Sigma^{(2)}$ and q is a scaling parameter referred to [33]. With the shared covariance structure as prior information (similar ideas of construction informative covariance priors can be found in [33]), the estimation is expected to be more accurate for certain parameters compared to the estimation made independently.

The covariance among the parameters for a single-printing process or 3-D printer can be estimated by using Algorithm 1. The estimated covariance will be used as the prior information for the parameter estimation of a new printing process.

With the informative priors on the parameters of different phases, the model estimation of different phases for a new printing process can be determined jointly via maximum a posterior (MAP) estimation. The covariance structure of all parameters $\{\theta_i\}_{i=1\ldots6}$ can be denoted as $\Theta^{(2)}$ and also captured by $\Theta^{(2)} \sim N(0, \Sigma^{(2)})$. The model parameters of these printers can be jointly estimated as follows:

$$\Theta^{(2)} = \arg\ \min \sum_{i=1}^{6} \frac{\left\| Y_i^{(2)} - X_i^{(2)}\theta_i^{(2)} - w^{(2)}(bp_{i-1}) \right\|_2^2}{\sigma_i^{2^{(2)}}} + \|\Theta^{(2)}\|_{\Sigma^{-1}}^2 \quad (4)$$

where $\|\ \|_Q^2$ stands for the weighted norm squared, e.g., $\|x\|_Q^2 = x^T Q x$. It should be noted that the first term is estimated by the data from printer 2 (target printer) and the information from source printer(s) is provided in the second term with an appropriate selection of norm and Σ that contributes to the learning for printer 2.

The solution to (4) can be obtained analytically. For example, if the scaling parameter q is selected to be 1 after numerical exploration, then (4) can be written as

$$\Theta^{(2)} = \arg\ \min \sum_{i=1}^{6} \left\| Y_i^{(2)} - X_i^{(2)}\theta_i^{(2)} - w^{(2)}(bp_{i-1}) \right\|_2^2 + \lambda\|\Theta^{(2)}\|_{\Sigma^{-1}}^2 \quad (5)$$

where λ can be regarded as a tuning parameter, which determines how fast to move the process variables from starting point to the endpoint on the task. However, the range of choosing λ should be specified by the user. Plenty of trials should be run to narrow the range and to obtain the λ for the most fitting model. One special case is that when $w^{(2)}(bp_{i-1})$ is the constant around some breakpoints, and there are only two segments p3 and p5 concerned, the solution to (5) can be simplified to

$$\Theta^{(2)} = \left(X_3^{(2)^T} X_3^{(2)} + X_5^{(2)^T} X_5^{(2)} + \lambda\Sigma^{-1}\right)^{-1} \times \left(X_3^{(2)^T} Y_3^{(2)} + X_5^{(2)^T} Y_5^{(2)}\right). \quad (6)$$

To summarize, the proposed informative prior-based transfer learning method has the following two key aspects.

1) The model parameters of different phases in the linewidth model are not independent. For example, the parameters may exhibit a multivariate normal distribution, i.e., $\{\alpha_1, \alpha_2, \beta, \gamma, c, \rho\} = \theta \sim N(\mu, \Sigma)$.
2) The covariance structure of the parameters is similar across different 3-D printers, which is the driving factor for transfer learning. For example, the covariance structures obtained from two 3-D printers may show the relationship of $\theta^{(1)} \sim N(0, \Sigma^{(1)})$ and $\theta^{(2)} \sim N(0, \Sigma^{(2)})$, where $\Sigma^{(1)} = q\Sigma^{(2)}$ and q is a scaling parameter.

Even if the piecewise kinematics-quality model is not the primary goal of this article, there is a lack of research that proposed a quantitative way of capturing kinematics conditions impact printing error. Only qualitative descriptions on such kinematics-induced printing error are available [18]–[20]. In addition, existing research on kinematic error modeling or calibration in FDM/FFF mostly focuses on the kinematic chain modeling in mechanical components, including the geometrical errors such as axis alignment, axis straightness, yaw, pitch, and roll [34] or machine errors such as zero error of the cable length and error of end-effector position [35]. However, these studies did not model the printing effect of the extruder kinematics affected by the parameters (e.g.,

TABLE II
PREDICTION RMSES FOR ALL THE EXPERIMENTS

Sample	1	2	3	4	5	6	7	8	9
RMSE	.068	.042	.034	.047	.047	.055	.041	.045	.030

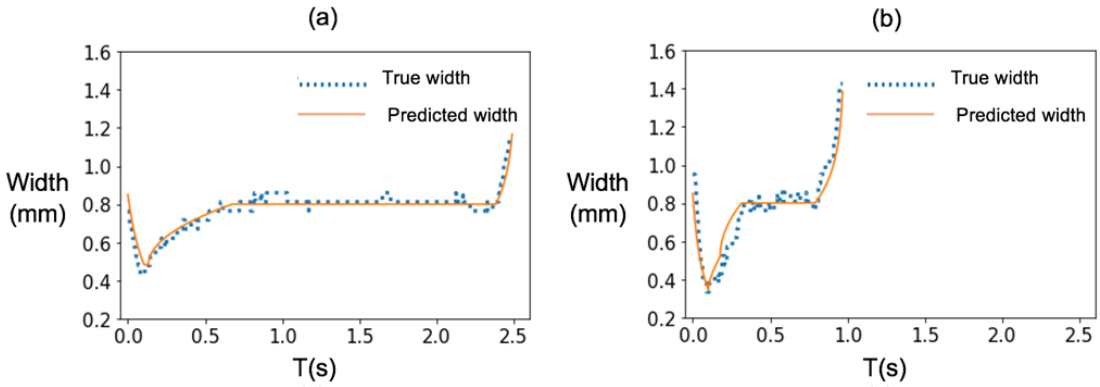

Fig. 6. Predicted width versus measurement values. Sample 9 at a speed (a) 50 mm/s has the smallest RMSE and sample 1 and (b) 150 mm/s has the largest RMSE. The printing times are different because the speed settings in the G-code are not the same.

printing speed/acceleration) from the G-code. This relationship can directly reveal the impact of G-code on printing quality, thereby enabling quality control by adjusting G-code by future research.

III. CASE STUDIES

The case study involves two extrusion-based 3-D printers, and each printer creates printing lines given different kinematics setups, as outlined in Table I. The quality data (printing linewidth) were obtained by processing the data from 2-D images captured by a high-resolution camera. The quality prediction model for estimating the printing linewidth variation and printed material distribution nonuniformity will be trained for one of the printers in case study A. In case study B, printer 2 is introduced, and it is assumed that many experimental data under the conditions in Table I are missing for this printer. Case B demonstrates how the between-printer transfer learning can help improve the modeling accuracy for the printer lacking sufficient data.

A. Case A: Printing Width Modeling for a Single-Printing Process

To test the performance of the model, we split the experiment data (see Table I) into the training and testing data. The split involves using eight experiment samples as the training data and the remaining 1 experiment sample as the testing data. This process is repeated nine times until each of all samples has been used as the testing data for once. The RMSE is used as the metric to evaluate the prediction performance. Table II summarizes the RMSE for all the nine cases. Fig. 6 shows the prediction results with the minimum and maximum RMSE. Based on the results, it can be concluded that the model can accurately capture the relationship between kinematic parameters and printing linewidth for quality prediction.

The printed lines are building elements for each layer in the printed structure. Although multiple printed lines often overlap to ensure the density of the printed block in some scenarios, the nonuniformity in the overlapped area still contributes to infill defects, mechanical strength problems, and surface height variation (surface shape and roughness). The infill nonuniformity can be estimated by applying the proposed model to multiple lines printed side-by-side. Fig. 7 shows the capability of the model estimating the printed material distribution nonuniformity. It can be seen that the model estimation can effectively capture the between-line gaps or void defects as well as nonuniform material overlap near the two ends of multiple infill lines.

B. Case B: Transfer Learning for a Data-Limited Printing Process

This study used common printer models, Lulzbot Taz 5 and Lulzbot Taz 6, based on Bowden extruders as an example to demonstrate the proposed transfer learning method. The printer Lulzbot Taz 5 serves as a data-rich source printer, whereas Lulzbot Taz 6 is the data-limited target printer in case study B. It should be noted that the methodology is still applicable to the transfer learning between different types of extrusion-based printer models. The same nine experiments, as shown in Table I, were conducted on LulzBot Taz 6. An example of one single-line printed linewidth is shown in Fig. 8, and other printing experiments exhibit similar changing patterns. It can be seen that the new printing process does not have the p1 phase as the previous printing process. The difference is caused by various factors, such as hardware/software upgrade on a different machine. However, this missing segment p1 does not affect the knowledge transfer regarding the correlation between other segments that both source and target printers have. The reason is that the correlation between two printing phases is independent

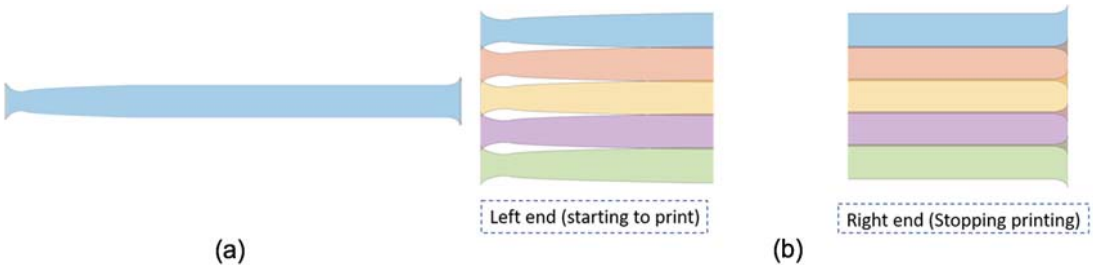

Fig. 7. (a) Estimated single-printed line. (b) Estimated multiple printed lines printed side-by-side at the two ends.

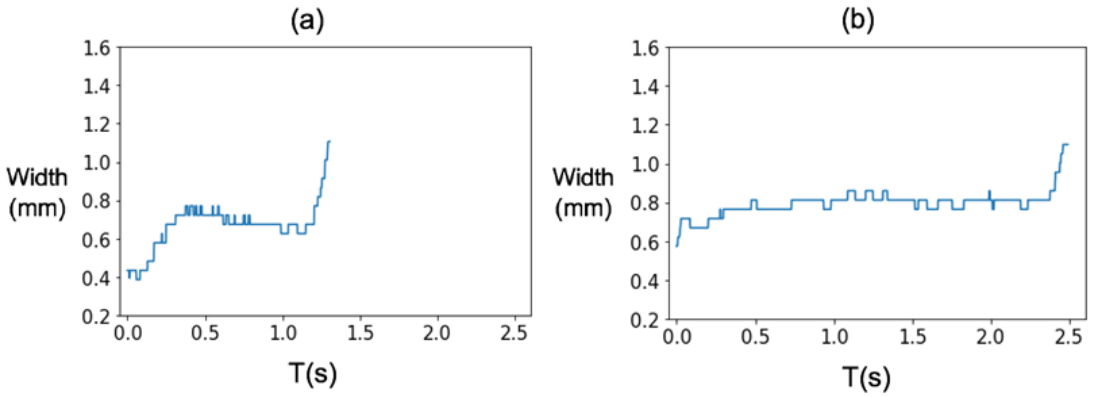

Fig. 8. Examples of printed linewidth from the target printer. (a) Printing results at a high printing speed of 150 mm/s. (b) Printing results at a low printing speed of 50 mm/s. The printing times are different because the speed settings in the G-code are not the same.

of other phases, as determined by extruder kinematics. The proposed model is still valid after removing the p1 part. As the p1 part is removed from the model, the breakpoint bp1 can be ignored.

To test the performance of the proposed informative prior-based transfer learning method, the following procedures were implemented.

1) Estimate the covariance of the parameters $\{\beta, \gamma, c, \rho\}$ using Algorithm 1 and the data from a data-rich printing process, i.e., the data from Case A.
2) Use the MAP method [see (4) and (5)] to estimate the parameters of the data-lacking printing process.

The data from Case A showed a significant positive covariance between γ and ρ. Therefore, the estimation of γ and ρ can be made jointly as (6).

Additional experimental data were obtained under nine different experimental conditions (G-codes) from the new printer. A subset of the data was added to the training data set in conjunction with the data in Case A. The remainder of the data from the new printer serves as the testing data. A cross-validation strategy is adopted to evaluate the performance of the transfer learning algorithm. For example, when the sample size in the training data from the new printer is one, the data obtained under one experimental condition (out of nine conditions) are chosen as the training data. The other eight experiments would be employed as the testing data. After exploiting all the possible training–testing combinations and collecting all the RSMEs from the measurements, the interquartile ranges of all RSMEs can be obtained for transfer learning and single-printer learning, respectively. All prediction RMSEs corresponding to the different sample sizes of training data from the target printer 2 are summarized in Fig. 9. Based on both the box plot [see Fig. 9(a)] and the median RMSE improvement percentage by transfer learning [see Fig. 9(b)] versus training sample size, it can be seen that the transfer learning leveraging source printer 1 can significantly improve the prediction accuracy, especially when the training sample size on printer 2 is very small.

C. Remark: Effectiveness of the Proposed Learning Method

Printing material, temperature, speed, and directions will jointly affect the transfer learning results by a complex mechanism. Though the mechanism is out of the scope of this study and the results can be significantly different, there are some general guidelines about the applicability of the proposed transfer learning method for the combined effects on the final quality. When the target printer is run at a higher printing speed and heated materials have a higher viscosity, a printed line exhibits a more significant pattern of piecewise thickening–thinning effect near the two ends of the line. If the pattern is more significant on the target printer, the learning results have better accuracy (lower RMSE) compared with single-printer learning. On the other hand, if the printing is performed at a very slow speed and material solidifies slow, the printed line tends to be more uniform, closer to the nominal geometry. The expected learning improvement is much limited. Such a difference is highlighted in Fig. 8. Therefore, the kinematics-based transfer learning has the great potential of improving prediction accuracy even if the target

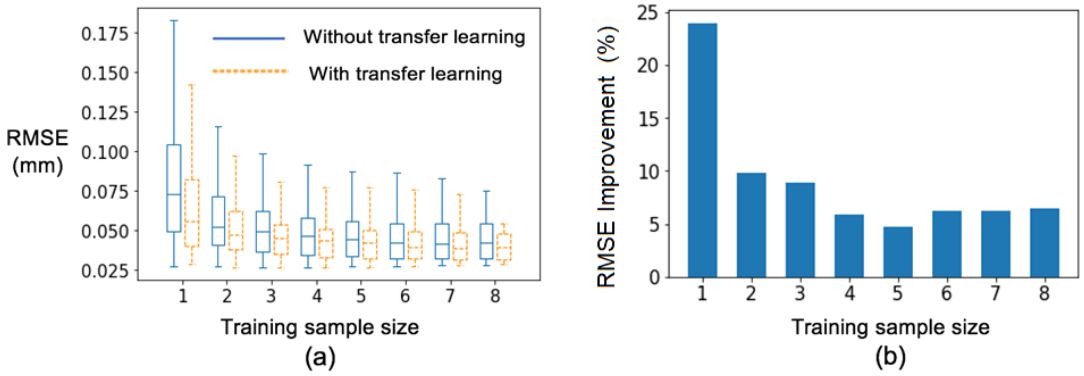

Fig. 9. Printing quality improvement using transfer learning. (a) Box plot of the prediction RMSE versus different sample sizes with/without transfer learning. (b) Median RMSE improvement percentage by transfer learning compared to without transfer learning versus different sample sizes in the training data.

and source printers use different materials and setup as long as two printers exhibit a significant piecewise pattern.

If multiple printing processes with different materials and setups are available, a printer screening and selection procedure can be adopted to identify, among candidates, the printer(s) that lead to the most significant RMSE reduction compared with single-printer learning. This data-driven printer selection can mitigate the potential negative knowledge transfer between printers with very different setups.

IV. Conclusion

In an extrusion-based AM process, the kinematic characteristics of a 3-D printer's extruder, such as acceleration and feed, can significantly impact the filling pattern of deposited materials, creating structural or surface defects, e.g., overfill/underfill problems. The defects of the material filling patterns can be caused by the geometric variations of each printing line. There is very limited research that quantitatively estimates the geometric variation of printing lines induced by extruder kinematics. The nonuniform material distribution is more commonly observed in interconnected collaborative printing systems since extruders make more start-to-end cycles. This article presents an initial step in addressing the material filling quality problem at two ends of each infill line by studying the effect of kinematic parameters on the geometric variations of each printing line. The main contributions of this article are twofold.

1) *Quantitative Understanding of the Impact of Kinematics on Printing Quality:* A data model based on a five-segment piecewise function guided by extruder kinematics was proposed to estimate the width of each printing line along the printing path given the kinematics setup as specified by a G-code. The model quantitatively reveals that the printing linewidth decreases as the extruder accelerates while increasing when the extruder reaches a constant speed. The linewidth further increases when the extruder decelerates when it approaches the end of a straight-line path or before the printing path direction changes. The single-line printing can contribute to the estimation of the printed material distribution of multiple infill lines and resultant infill defects.
2) *Interpretable Between-Printer Transfer Learning for Quick Training of the Quality Model for Process Control:* The training of the established model parameters requires sufficient historical data; however, it can be time-consuming and costly to test the printing quality for many kinematics setups (G-code) in real-world production. This article employs the proposed model structure to explore the similar variation patterns between two similar-but-nonidentical printers with historical data. Also, the proposed transfer learning method is not limited to specific printer models. Based on the similarity in the covariance structure among the model parameters, a between-printer transfer learning algorithm is developed to supplement among interconnected printers (e.g., from one data-rich printer to another with limited data) to improve the learning accuracy of model parameters via MAP estimation. Compared with traditional transfer learning that used a generic kernel or norm function to capture the relatedness among multiple data sources, this study provides an interpretable way of characterizing between-printer relatedness as the similar impacts of extruder kinematics on printing line geometric variations. Thus, the method can simplify the model structures to facilitate learning compared with data-driven transfer learning.
3) *Reduction of Calibration and Ramp-Up for Flexible Production:* The proposed between-printer transfer learning can effectively reduce the printer calibration efforts and process ramp-up when a (new) printer is engaged with a new printing task by leveraging other printers' experiences. This method can reduce the testing effort for a target printer to understand how printing conditions specified in G-code can affect printing quality when new material and process setup is adopted by new printing tasks. Therefore, between-printer transfer learning is very suitable for the scalable production of a high variety of parts in small batches with frequent printing task changes.

The effectiveness of the method was demonstrated by experimental studies using two extrusion-based 3-D printers. The results indicated that: 1) the model has shown its capability in making informative predictions of printing line variation and nonuniform material distribution of multiple infill lines and

2) the transfer learning can improve the modeling accuracy. The case studies show that when the sample size is only 1–2, the prediction by single-printer learning is significantly worse than the transfer learning approach by up to 24%. When the sample size grows larger, the performance of model training with and without using the transfer learning algorithm is close.

The proposed approach is limited to the quality prediction for straight-line printing errors induced by kinematics. In addition, the method requires source printers to have relatively sufficient data to compute an estimate of the covariance structure. Thus, the method performs better for transfer learning from data-rich source printer(s) to a data-limited target printer.

V. Future Work

Future research and applications include the following.

1) *Printing Quality Control for Mass Personalization:* The value of this article lies in the reduction of potential calibration efforts for a reconfigurable printing system that deals with a high variety of products in different shapes/sizes with different materials. When printing a new product with different materials and geometry or a new printer is engaged in collaborative printing tasks, the printer must be calibrated/recalibrated to reduce the printing errors. Such calibrations for different printing tasks require frequent trial-and-error tests under different kinematics setups, thus significantly jeopardizing the printing efficiency and prolonging the ramp-up time for new printing task. The small-batch production of a high variety of parts is most important for the future manufacturing of personalized products.
2) *Co-Learning Among Multiple Data-Limited Printers:* The between-printer transfer learning strategy in this article can be extended to the multiprinter co-learning in future research. However, two major challenges could be concerned: 1) the learning-useless source printers might lower the learning performance once they are involved. 2) The covariance may not be reliable or derivable when multiple printers are available, each carrying very limited data. Thus, developing a printing process selection algorithm is necessary for the target printer to efficiently improve the effectiveness of knowledge transfer. Furthermore, the shared parameter covariance structure can be learned jointly by multiple data-limited printers. Such a co-learning strategy to be developed in the future does not necessarily require a data-rich printer and can allow for joint training of the quality prediction model based on common covariance structures.
3) *Reducing Infill Defects by Adjusting G-Codes:* The model prediction in this research can be employed to evaluate the material filling quality in the final product and guide the planning of G-code by varying the feed and extrusion rate to offset potential printing errors. The outcome of this research can improve the efficiency of collaborative AM for high-efficient production for customization.

Acknowledgment

This research is conducted at the High-Performance Materials Institute (HPMI), FAMU-FSU College of Engineering. The authors would like to thank Dr. Tarik Dickens, HPMI, for assistance.

References

[1] A. Dey and N. Yodo, "A systematic survey of FDM process parameter optimization and their influence on part characteristics," *J. Manuf. Mater. Process.*, vol. 3, no. 3, p. 64, Jul. 2019.
[2] K. He, Q. Zhang, and Y. Hong, "Profile monitoring based quality control method for fused deposition modeling process," *J. Intell. Manuf.*, vol. 30, no. 2, pp. 947–958, Feb. 2019.
[3] R. Leal *et al.*, "Additive manufacturing tooling for the automotive industry," *Int. J. Adv. Manuf. Technol.*, vol. 92, nos. 5–8, pp. 1671–1676, 2017.
[4] M. Khanzadeh, P. Rao, R. Jafari-Marandi, B. K. Smith, M. A. Tschopp, and L. Bian, "Quantifying geometric accuracy with unsupervised machine learning: Using self-organizing map on fused filament fabrication additive manufacturing parts," *J. Manuf. Sci. Eng.*, vol. 140, no. 3, Mar. 2018.
[5] L. Cheng, A. Wang, and F. Tsung, "A prediction and compensation scheme for in-plane shape deviation of additive manufacturing with information on process parameters," *IISE Trans.*, vol. 50, no. 5, pp. 394–406, May 2018.
[6] J. Liu, C. Liu, Y. Bai, P. Rao, C. B. Williams, and Z. Kong, "Layer-wise spatial modeling of porosity in additive manufacturing," *IISE Trans.*, vol. 51, no. 2, pp. 109–123, Feb. 2019.
[7] R. de Souza Borges Ferreira, A. Sabbaghi, and Q. Huang, "Automated geometric shape deviation modeling for additive manufacturing systems via Bayesian neural networks," *IEEE Trans. Autom. Sci. Eng.*, vol. 17, no. 2, pp. 584–598, Apr. 2020.
[8] Q. Huang, Y. Wang, M. Lyu, and W. Lin, "Shape deviation generator—A convolution framework for learning and predicting 3-D printing shape accuracy," *IEEE Trans. Autom. Sci. Eng.*, vol. 17, no. 3, pp. 1486–1500, Jul. 2020.
[9] A. Wang, S. Song, Q. Huang, and F. Tsung, "In-plane shape-deviation modeling and compensation for fused deposition modeling processes," *IEEE Trans. Autom. Sci. Eng.*, vol. 14, no. 2, pp. 968–976, Apr. 2017.
[10] K. Tong, S. Joshi, and E. Amine Lehtihet, "Error compensation for fused deposition modeling (FDM) machine by correcting slice files," *Rapid Prototyping J.*, vol. 14, no. 1, pp. 4–14, Jan. 2008.
[11] A. Noriega, D. Blanco, B. J. Alvarez, and A. Garcia, "Dimensional accuracy improvement of FDM square cross-section parts using artificial neural networks and an optimization algorithm," *Int. J. Adv. Manuf. Technol.*, vol. 69, nos. 9–12, pp. 2301–2313, Dec. 2013.
[12] L. M. Galantucci, I. Bodi, J. Kacani, and F. Lavecchia, "Analysis of dimensional performance for a 3D open-source printer based on fused deposition modeling technique," *Procedia CIRP*, vol. 28, pp. 82–87, Dec. 2015.
[13] F. Górski, W. Kuczko, and R. Wichniarek, "Influence of process parameters on dimensional accuracy of parts manufactured using fused deposition modelling technology," *Adv. Sci. Technol.-Res. J.*, vol. 7, no. 19, pp. 27–35, Sep. 2013.
[14] A. Equbal, A. K. Sood, A. R. Ansari, and A. Equbal, "Optimization of process parameters of fdm part for minimiizing its dimensional inaccuracy," *Int. J. Mech. Prod. Eng. Res. Develop.*, vol. 7, no. 2, pp. 57–66, 2017.
[15] M. Shojib Hossain, D. Espalin, J. Ramos, M. Perez, and R. Wicker, "Improved mechanical properties of fused deposition modeling-manufactured parts through build parameter modifications," *J. Manuf. Sci. Eng.*, vol. 136, no. 6, pp. 061002-1–061002-12, Dec. 2014, doi: 10.1115/1.4028538.
[16] L. Li, A. Haghighi, and Y. Yang, "Theoretical modelling and prediction of surface roughness for hybrid additive–subtractive manufacturing processes," *IISE Trans.*, vol. 51, no. 2, pp. 124–135, Feb. 2019.
[17] H. Sun, P. K. Rao, Z. J. Kong, X. Deng, and R. Jin, "Functional quantitative and qualitative models for quality modeling in a fused deposition modeling process," *IEEE Trans. Autom. Sci. Eng.*, vol. 15, no. 1, pp. 393–403, Jan. 2018.
[18] M. K. Agarwala, V. R. Jamalabad, N. A. Langrana, A. Safari, P. J. Whalen, and S. C. Danforth, "Structural quality of parts processed by fused deposition," *Rapid Prototyping J.*, vol. 2, no. 4, pp. 4–19, Dec. 1996.

[19] A. Bouhal, M. A. Jafari, W.-B. Han, and T. Fang, "Tracking control and trajectory planning in layered manufacturing applications," *IEEE Trans. Ind. Electron.*, vol. 46, no. 2, pp. 445–451, Apr. 1999.

[20] A. Bellini, S. Guáeri, and M. Bertoldi, "Liquefier dynamics in fused deposition," *J. Manuf. Sci. Eng.*, vol. 126, no. 2, pp. 237–246, May 2004.

[21] P. Ravi, P. S. Shiakolas, and A. Dnyaneshwar Thorat, "Analyzing the effects of temperature, nozzle-bed distance, and their interactions on the width of fused deposition modeled struts using statistical techniques toward precision scaffold fabrication," *J. Manuf. Sci. Eng.*, vol. 139, no. 7, Jul. 2017, Art. no. 071007.

[22] Q. Qin, J. Huang, and J. Yao, "A real-time adaptive look-ahead speed control algorithm for FDM-based additive manufacturing technology with Hbot kinematic system," *Rapid Prototyping J.*, vol. 25, no. 6, pp. 1095–1107, Jul. 2019.

[23] L. Santana, C. H. Ahrens, A. da Costa Sabino Netto, and C. Bonin, "Evaluating the deposition quality of parts produced by an open-source 3D printer," *Rapid Prototyping J.*, vol. 23, no. 4, pp. 796–803, Jun. 2017.

[24] R. Comminal, M. P. Serdeczny, D. B. Pedersen, and J. Spangenberg, "Numerical modeling of the strand deposition flow in extrusion-based additive manufacturing," *Additive Manuf.*, vol. 20, pp. 68–76, Mar. 2018.

[25] L. Cheng, F. Tsung, and A. Wang, "A statistical transfer learning perspective for modeling shape deviations in additive manufacturing," *IEEE Robot. Autom. Lett.*, vol. 2, no. 4, pp. 1988–1993, Oct. 2017.

[26] L. Cheng, K. Wang, and F. Tsung, "A hybrid transfer learning framework for in-plane freeform shape accuracy control in additive manufacturing," *IISE Trans.*, vol. 53, no. 2, pp. 298–312, 2020.

[27] A. Sabbaghi, Q. Huang, and T. Dasgupta, "Bayesian model building from small samples of disparate data for capturing in-plane deviation in additive manufacturing," *Technometrics*, vol. 60, no. 4, pp. 532–544, Oct. 2018.

[28] A. Sabbaghi and Q. Huang, "Model transfer across additive manufacturing processes via mean effect equivalence of lurking variables," *Ann. Appl. Statist.*, vol. 12, no. 4, pp. 2409–2429, Dec. 2018.

[29] J. Francis, A. Sabbaghi, M. Ravi Shankar, M. Ghasri-Khouzani, and L. Bian, "Efficient distortion prediction of additively manufactured parts using Bayesian model transfer between material systems," *J. Manuf. Sci. Eng.*, vol. 142, no. 5, May 2020.

[30] S. Jialin Pan and Q. Yang, "A survey on transfer learning," *IEEE Trans. Knowl. Data Eng.*, vol. 22, no. 10, pp. 1345–1359, Oct. 2010.

[31] L. Poudel, C. Blair, J. McPherson, Z. Sha, and W. Zhou, "A heuristic scaling strategy for multi-robot cooperative three-dimensional printing," *J. Comput. Inf. Sci. Eng.*, vol. 20, no. 4, pp. 041002-1–041002-12, Aug. 2020, doi: 10.1115/1.4045143.

[32] H. Shen, L. Pan, and J. Qian, "Research on large-scale additive manufacturing based on multi-robot collaboration technology," *Additive Manuf.*, vol. 30, Dec. 2019, Art. no. 100906.

[33] R. Raina, A. Y. Ng, and D. Koller, "Constructing informative priors using transfer learning," in *Proc. 23rd Int. Conf. Mach. Learn. (ICML)*, 2006, pp. 713–720.

[34] S. Keaveney, P. Connolly, and E. D. O'Cearbhaill, "Kinematic error modeling and error compensation of desktop 3D printer," *Nanotechnol. Precis. Eng.*, vol. 1, no. 3, pp. 180–186, Sep. 2018.

[35] S. Qian, K. Bao, B. Zi, and N. Wang, "Kinematic calibration of a cable-driven parallel robot for 3D printing," *Sensors*, vol. 18, no. 9, p. 2898, Sep. 2018.

Jie Ren received the B.S. degree in industrial engineering from Shanghai Jiao Tong University, Shanghai, China, in 2014, and the Ph.D. degree in industrial engineering from Florida State University, Tallahassee, FL, USA, in 2019.

His research focuses on spatial data modeling and machine learning with applications to engineering systems.

An-Tsun Wei received the B.B.A. degree in logistics management from the National Kaohsiung University of Science and Technology, Kaohsiung, Taiwan, in 2015, and the M.S. degree in industrial engineering from Florida State University, Tallahassee, FL, USA, in 2019, where he is currently pursuing the Ph.D. degree in industrial engineering.

His research focuses on machine learning with application to additive manufacturing.

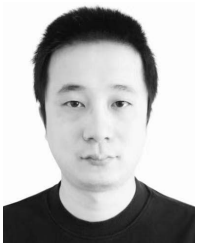

Zhengqian Jiang received the B.S. degree in mechanical engineering manufacture and automatization from the China University of Petroleum, Beijing, China, in 2010, the M.S. degree in aerospace engineering from Shanghai Jiao Tong University, Shanghai, China, in 2013, and the M.S. and Ph.D. degrees in industrial engineering from Florida State University, Tallahassee, FL, USA, in 2015 and 2020, respectively.

He is currently a Research Scientist at Amazon, Bellevue, WA, USA. His research focuses on manufacturing systems modeling and supply chain optimization.

Hui Wang received the Ph.D. degree in industrial engineering from the University of South Florida, Tampa, FL, USA, in 2007.

He is currently an Associate Professor of industrial and manufacturing engineering at the College of Engineering, Florida A&M University-Florida State University, Tallahassee, FL, USA. His research has been focused on engineering system modeling, data analytics, and optimization to support quality control and manufacturing system design.

Xiaolin Wang received the B.E. degree in polymer science and engineering from Sichuan University, Chengdu, China, in 2014, and the M.Sc. degree in material science from Washington State University, Pullman, WA, USA, in 2016. He is currently pursuing the Ph.D. degree in industrial and manufacturing engineering with Florida State University, Tallahassee, FL, USA.

His research focuses on the fabrication of piezoelectric polymer foam via additive manufacturing.